

Effect of Ni substitution on the formability and magnetic properties of $Gd_{50}Co_{50}$ amorphous alloy

Ben-Zheng Tang(唐本镇), Xiao-Ping Liu(刘晓萍), Dong-Mei Li(李冬梅), Peng Yu(余鹏), Lei Xia(夏雷)
Citation: Chin. Phys. B . 2020, 29(5): 056401 . **doi:** 10.1088/1674-1056/ab7da8
Journal homepage: http://cpb.iphy.ac.cn; http://iopscience.iop.org/cpb

What follows is a list of articles you may be interested in

Ab initio molecular dynamics simulations of nano-crystallization of Fe-based amorphous alloys with early transition metals

Yao-Cen Wang(汪姚岑), Yan Zhang(张岩), Yoshiyuki Kawazoe, Jun Shen(沈军), Chong-De Cao(曹崇德)
Chin. Phys. B . 2018, 27(11): 116401 . **doi:** 10.1088/1674-1056/27/11/116401

Secondary relaxation and dynamic heterogeneity in metallic glasses: A brief review

J C Qiao(乔吉超), Q Wang, D Crespo, Y Yang(杨勇), J M Pelletier
Chin. Phys. B . 2017, 26(1): 016402 . **doi:** 10.1088/1674-1056/26/1/016402

Interstitialcy theory of condensed matter states and its application to non-crystalline metallic materials

V A Khonik
Chin. Phys. B . 2017, 26(1): 016401 . **doi:** 10.1088/1674-1056/26/1/016401

Large reversible magnetocaloric effect induced by metamagnetic transition in antiferromagnetic HoNiGa compound

Yi-Xu Wang(王一旭), Hu Zhang(张虎), Mei-Ling Wu(吴美玲), Kun Tao(陶坤), Ya-Wei Li(李亚伟), Tim Yan(颜天宝), Ke-Wen Long(龙克文), Teng Long(龙腾), Zheng Pang(庞铮), Yi Long(龙毅)
Chin. Phys. B . 2016, 25(12): 127104 . **doi:** 10.1088/1674-1056/25/12/127104

Coexistence of positive and negative magnetic entropy changes in $CeMn_2(Si_{1-x}Ge_x)_2$ compounds

Zuo Wen-Liang, Hu Feng-Xia, Sun Ji-Rong, Shen Bao-Gen
Chin. Phys. B . 2015, 24(9): 097104 . **doi:** 10.1088/1674-1056/24/9/097104

Effect of Ni substitution on the formability and magnetic properties of $Gd_{50}Co_{50}$ amorphous alloy*

Ben-Zheng Tang(唐本镇)[1,2], Xiao-Ping Liu(刘晓萍)[1], Dong-Mei Li(李冬梅)[1], Peng Yu(余鹏)[1,†], and Lei Xia(夏雷)[2]

[1] *Chongqing Key Laboratory of Photo-Electric Functional Materials, College of Physics and Electronic Engineering, Chongqing Normal University, Chongqing* 401331, *China*

[2] *Laboratory for Microstructure & Institute of Materials, Shanghai University, Shanghai* 200072, *China*

(Received 10 February 2020; revised manuscript received 25 February 2020; accepted manuscript online 9 March 2020)

A small amount of Ni was added into the binary $Gd_{50}Co_{50}$ amorphous alloy to replace Gd in order to obtain ternary $Co_{50}Gd_{50-x}Ni_x$ ($x = 1$, 2, and 3) amorphous alloys. Compared to the binary $Gd_{50}Co_{50}$ amorphous alloy, the $Co_{50}Gd_{50-x}Ni_x$ amorphous alloys show an enhanced Curie temperature (T_C) with a weakened formability. The maximum magnetic entropy change ($-\Delta S_m^{peak}$) of the $Co_{50}Gd_{50-x}Ni_x$ amorphous alloys is found to decrease with the increasing T_C. The adiabatic temperature rise (ΔT_{ad}) of the $Co_{50}Gd_{47}Ni_3$ amorphous alloy is superior to that of the Fe-based metallic glasses at room temperature. The variation of the T_C and $-\Delta S_m^{peak}$ of the $Gd_{50}Co_{50}$ amorphous alloy with Ni addition, and the mechanism involved, were discussed.

Keywords: amorphous alloy, glass forming ability, magnetocaloric effect, adiabatic temperature rise

PACS: 64.70.pe, 71.23.Cq, 75.30.Sg **DOI:** 10.1088/1674-1056/ab7da8

1. Introduction

Energy efficiency and environmentally friendliness have become the most urgent requirement of refrigeration technology due to the increasing energy shortage and environmental deterioration. Therefore, efforts have been made to develop new climate-friendly refrigeration solutions with high efficiency. The magnetic refrigeration (MR) technology, by using the endothermic and exothermic characteristic of a refrigerating medium upon the variation of the magnetic field, has displayed promising potential due to its compactness, high efficiency, energy saving, and environmental harmlessness.[1–5]

As the working materials play a critical role in the efficiency of the magnetic refrigerator, numerous magnetic alloys that exhibit fine magneto-caloric effect (MCE) have been studied intensively in recent years.[5–25] Amongst these MCE materials, the amorphous alloys display better mechanical properties and corrosion resistance, in addition to their excellent magnetic proprieties. For instance, the Gd-based amorphous alloys show considerable prospects as magnetic refrigerants based on their soft magnetic performance with negligible magnetic hysteresis at different temperatures, the ultrahigh refrigeration capacity (*RC*) corresponding to their broadened magnetic entropy change ($-\Delta S_m$) peak, and especially their tunable Curie temperature (T_C) over a wide range of composition.

However, as the situation in the Gd–Co binary metallic glasses,[23–25] the glass formability (GFA) and MCE of the Gd-based amorphous alloys become worse with the increasing T_C.[8–22] Therefore, although the multicomponent Gd-based bulk metallic glasses show high glass formability and outstanding MCE at low temperature, the Gd-based amorphous alloys can only be fabricated into thin ribbons when improving the T_C to near the room temperature and their maximum magnetic entropy change ($-\Delta S_m^{peak}$) is usually less than half of the $-\Delta S_m^{peak}$ value of pure Gd. So far, the T_C of the Gd-based fully amorphous alloys is lower than 282 K, which makes it difficult to compose the amorphous composites with a table-like $-\Delta S_m$ profile suitable for a magnetic refrigeration cycle of a domestic refrigerator or air conditioner. In this work, through adding a small amount of Ni to substitute Gd of the binary $Gd_{50}Co_{50}$ amorphous alloy, we obtain $Co_{50}Gd_{50-x}Ni_x$ alloys in an attempt to achieve improved formability and enhanced T_C, without excessive reduction the MCE of the initial alloy. The thermal and magnetic properties of the $Co_{50}Gd_{50-x}Ni_x$ ($x = 1$, 2, and 3) amorphous alloys were measured. Based on the experimental results obtained from these Ni addition samples, the change of the formability, T_C, as well as the $-\Delta S_m^{peak}$ compared to the $Gd_{50}Co_{50}$ amorphous alloy were investigated. The adiabatic temperature rise (ΔT_{ad}) was calculated to assess the application perspective as a magnetic refrigerant around room temperature.

2. Experimental procedures

Samples with nominal compositions of $Co_{50}Gd_{50-x}Ni_x$ ($x = 1$, 2, 3, 4, and 5) were firstly prepared into ingots by arc-

*Project supported by the National Natural Science Foundation of China (Grant Nos. 51671119 and 51871139), the Chongqing Research Program of Basic Research and Frontier Technology, China (Grant No. cstc2018jcyjAX0329 and cstc2018jcyjAX0444), and the Key Project of Science and Technology Research Program of Chongqing Education Commission of China (Grant No. KJZD-K201900501).

†Corresponding author. E-mail: pengyu@cqnu.edu.cn

© 2020 Chinese Physical Society and IOP Publishing Ltd

melting of pure Gd, Co, and Ni metals (purity $\geq$ 99.9 at.%) for several times under a Ti-gettered Ar atmosphere, and then quenched into ribbons with a thickness of 30–40 μm by a single roller melt-spinning method. The structural characteristics of the as-spun ribbons were tested by the Rigaku x-ray diffraction (XRD, model D\max-2550) using Cu K_α radiation. The thermal properties of the amorphous ribbons were obtained from the differential scanning calorimetry (DSC) curves measured by a Perkin-Elmer calorimeter (DIAMOND) at a heating rate of 20 K/min. The temperature dependence of magnetization (M–T) curves and the isothermal magnetization (M–H) curves were measured in a Quantum Design physical properties measurement system (PPMS, model 6000), and the magnetic proprieties of Curie temperature (T_C) and magnetic entropy change ($-\Delta S_m$) were calculated from the M–T and M–H curves accordingly.

3. Results and discussion

Figure 1 shows XRD patterns of as-spun $Co_{50}Gd_{50-x}Ni_x$ (x = 1, 2, 3, 4, and 5) ribbons. The $Co_{50}Gd_{50-x}Ni_x$ (x = 1, 2, and 3) as-spun ribbons display a representative amorphous characteristic with a broad diffraction hump and no obvious crystalline peaks in their XRD patterns. In contrast, the $Co_{50}Gd_{46}Ni_4$ as-spun ribbon is partially crystalline and the $Co_{50}Gd_{45}Ni_5$ as-spun ribbon is almost fully crystalline as their XRD patterns appear obvious crystalline peaks of Gd_2Co phase.

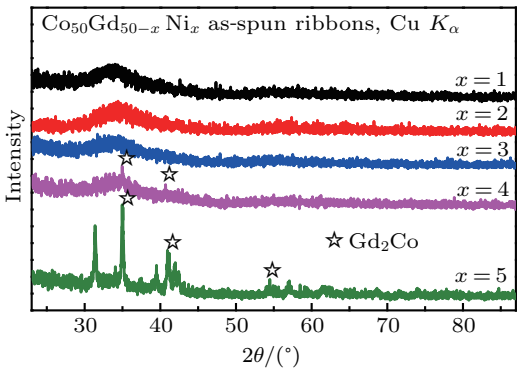


Fig. 1. XRD patterns of the as-spun ribbons of $Co_{50}Gd_{50-x}Ni_x$ (x = 1, 2, 3, 4, and 5).

DSC measurements under a heating rate of 20 K/min were performed to obtain the thermodynamic parameters of the $Co_{50}Gd_{50-x}Ni_x$ (x = 1, 2, and 3) amorphous ribbons. As shown in Fig. 2, the DSC curves of the $Co_{50}Gd_{50-x}Ni_x$ glassy ribbons exhibit a typical endothermic reaction before the sharp exothermic peaks of crystallization, which further indicates the glassy structure of the alloys. The glass transition temperature T_g, the liquidus temperature T_l, and the crystallization temperature T_x obtained from the DSC curves are listed in Table 1. It is found that the T_g and T_l of the $Co_{50}Gd_{50}$ amorphous alloy get increased with Ni substituting the Gd elements, which is most likely ascribed to the introduced 3d–3d direct exchange interactions stronger than the indirect interactions from Gd. While the calculated supercooled liquid region ΔT_x ($\Delta T_x = T_x - T_g$) that is used to indicate the thermal stability of the supercooled liquids becomes narrow with Ni addition. It may be related to the reduction of the 3d–4f indirect exchange interactions caused by the replacement of Gd. As is well known, the f–d hybridization stabilizes the supercooled liquid or the glass against crystallization by the localization of the electrons,[26,27] and as a result, the reduced 3d–4f interactions in the $Co_{50}Gd_{50-x}Ni_x$ amorphous alloys will weaken the f–d hybridization, thereby broken the stable state of the undercooled liquids and deteriorate their glass-forming ability (GFA). According to the DSC results and the above analysis, the substitution of 1 at.% Ni hardly affects the thermal stability and GFA of the alloy, while the substitution of 2–3 at.% Ni weakens the corresponding thermal stability and GFA, which is well consistent with the results of XRD.

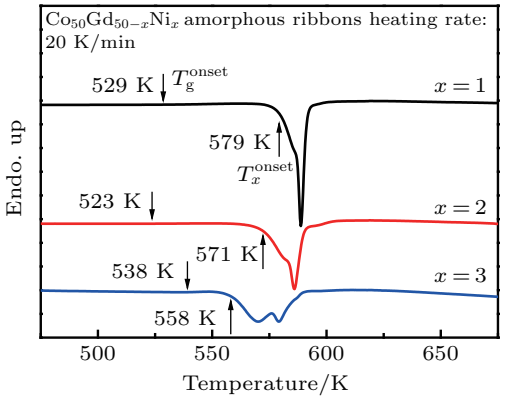


Fig. 2. DSC traces of the $Co_{50}Gd_{50-x}Ni_x$ (x = 1, 2, and 3) amorphous ribbons obtained at a heating rate of 20 K/min.

Figure 3(a) shows the hysteresis loops of the $Co_{50}Gd_{50-x}Ni_x$ (x = 1, 2, and 3) amorphous ribbons measured at 10 K and 350 K under a field of 5 T. The amorphous ribbon is ferromagnetic at 10 K and becomes paramagnetic at room temperature. The saturation magnetization (M_s) is about 166 A·m^2/kg for $Co_{50}Gd_{49}Ni_1$, 159 A·m^2/kg for $Co_{50}Gd_{48}Ni_2$, and 153 A·m^2/kg for $Co_{50}Gd_{47}Ni_3$, respectively. Therefore, the $-\Delta S_m^{peak}$ of the $Co_{50}Gd_{49}Ni_1$ amorphous ribbon is expected to be slightly higher than that of the $Co_{50}Gd_{48}Ni_2$ and $Co_{50}Gd_{47}Ni_3$ amorphous ribbons because $-\Delta S_m^{peak}$ is closely related to the M_s of the amorphous alloys.

The M–T curves of the $Co_{50}Gd_{50-x}Ni_x$ (x = 1, 2, and 3) metallic glasses were measured to reveal the magnetic transition temperature of the alloys. The Curie temperature T_C, as shown in Fig. 3(b), is about 273 K for $Co_{50}Gd_{49}Ni_1$, increased to 280 K for $Co_{50}Gd_{48}Ni_2$, and improved to 289 K for $Co_{50}Gd_{47}Ni_3$. Therefore, through adding Ni to the binary $Gd_{50}Co_{50}$ amorphous alloy to reduce the Gd content, the Curie

temperature of the $Co_{50}Gd_{50-x}Ni_x$ amorphous alloys is successfully improved to a higher temperature, especially, T_C of the $Co_{50}Gd_{47}Ni_3$ amorphous ribbon is higher than that of most Gd-based amorphous alloys.[8–25]

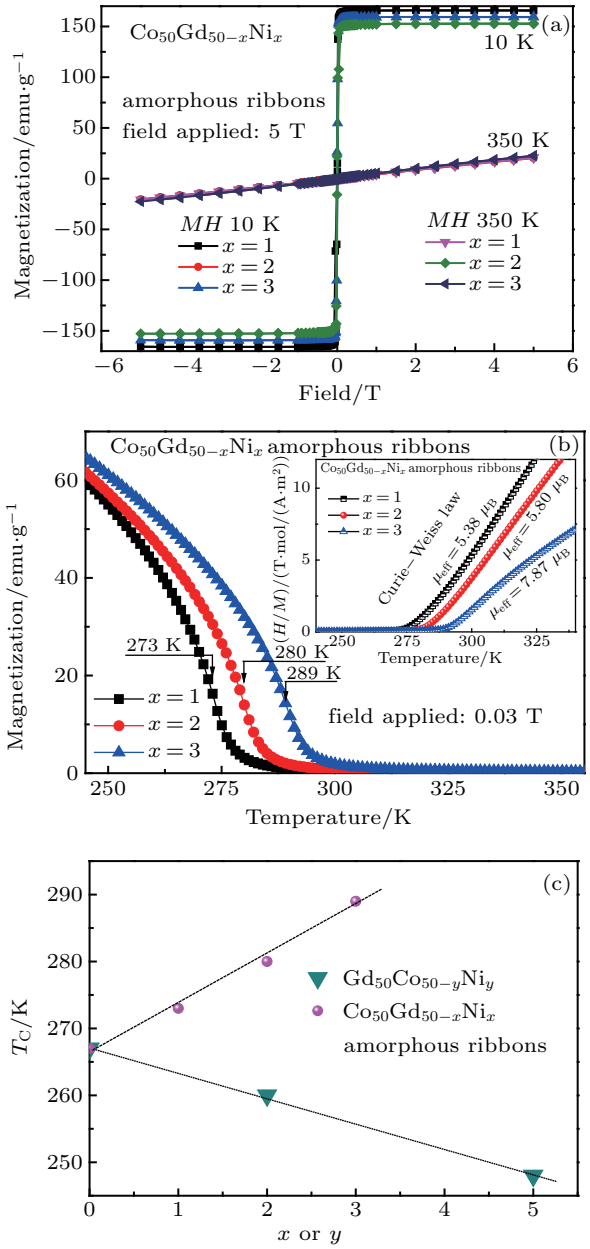


Fig. 3. (a) The hysteresis loops of the $Co_{50}Gd_{50-x}Ni_x$ ($x = 1$, 2, and 3) amorphous ribbons measured at 10 K and 350 K under a field of 5 T. (b) The M–T curves of the $Co_{50}Gd_{50-x}Ni_x$ ($x = 1$, 2, and 3) amorphous ribbons under a field of 0.03 T, the inset is μ_{eff} of the amorphous alloys. (c) Compositional dependence of T_C for the $Co_{50}Gd_{50-x}Ni_x$ ($x = 1$, 2, and 3) and $Gd_{50}Co_{50-y}Ni_y$ ($y = 2$ and 5) amorphous alloys.

In order to investigate the mechanism for the improvement of the magnetic transition temperature of the $Co_{50}Gd_{50-x}Ni_x$ ($x = 1$, 2, and 3) amorphous alloys, we constructed the compositional dependence of T_C for the $Co_{50}Gd_{50-x}Ni_x$ amorphous alloys, as shown in Fig. 3(c). For comparison, the relationship between the composition and T_C for the $Gd_{50}Co_{50-y}Ni_y$ ($y = 2$ and 5) amorphous alloys is also illustrated in Fig. 3(c). The T_C of the $Co_{50}Gd_{50-x}Ni_x$ amorphous alloys increases from 267 K for $Co_{50}Gd_{50}$, to 273 K for $Co_{50}Gd_{49}Ni_1$, 280 K for $Co_{50}Gd_{48}Ni_2$, and to 289 K for $Co_{50}Gd_{47}Ni_3$. In contrast, the T_C of the $Gd_{50}Co_{50-y}Ni_y$ ($y = 2$ and 5) amorphous alloys decreases from 267 K for $y = 0$ to 260 K for $y = 2$ and to 248 K for $y = 5$.

It is common that in the Gd–(TM)-based amorphous alloys, there exist at least three kinds of interactions between the matrix elements: the direct 3d–3d electronic interaction between the transition elements that contain the unfilled 3d shell and the indirect coupling of 4f–4f electronic interaction form the RE elements. Besides the respective interactions of the compositional elements themselves, there also exists the 3d–4f interaction between the different atoms. Referring to the previous research on the Gd–TM amorphous alloys,[14,25] the 3d–4f indirect interaction is considered to be negligible compared with other interactions in determining the Curie temperature of the samples. Therefore, for $Gd_{50}Co_{50-y}Ni_y$ ($x = 2$ and 5) amorphous alloys with a constant proportion of RE elements, the changed T_C of the alloys should have little relation with the RE interactions and could be mainly ascribed to the 3d–3d direct interaction between the transition metals.[20] On the other hand, the decreasing T_C with Ni content in the $Gd_{50}Co_{50-y}Ni_y$ ($y = 2$ and 5) amorphous alloys is understandable because the magnetic moment of Ni is smaller than that of Co, which means the reduced 3d–3d interactions between the transition metals. The effect of Ni substitution on the T_C of the $Co_{50}Gd_{50-x}Ni_x$ metallic glasses, however, is more complicated. The nominal magnetic moment ($\mu_{nom.}$) of the $Co_{50}Gd_{50-x}Ni_x$ amorphous alloys decreases from $6.352\mu_B$ for $x = 1$, to $6.302\mu_B$ for $x = 2$ and to $6.256\mu_B$ for $x = 3$ because the magnetic moment of Ni is much smaller than that of Gd. However, the effective magnetic moment (μ_{eff}) calculated according to the Curie–Weiss law, as shown in the inset of Fig. 3(b), increases from $5.38\mu_B$ for $x = 1$, to $5.8\mu_B$ for $x = 2$ and to $7.87\mu_B$ for $x = 3$. The increasing μ_{eff} implies that the Ni substitution for Gd enhances the magnetic interactions with the increasing Ni concentration. According to the results obtained from the Gd–Ni binary amorphous alloy system,[14] the interactions between Gd–Gd and Gd–Ni in the system are similar to each other in determining the T_C. Therefore, for the $Co_{50}Gd_{50-x}Ni_x$ amorphous alloys with constant Co concentration, the Co–Co interactions are almost unchanged, and thus, the enhanced magnetic interaction and the improved T_C with Ni addition in the $Co_{50}Gd_{50-x}Ni_x$ amorphous ribbons are probably ascribed to the additional 3d–3d coupling from the Co–Ni interactions.

The temperature dependence curves of $-\Delta S_m$ under various magnetic fields of the $Co_{50}Gd_{50-x}Ni_x$ amorphous alloys were obtained by measuring the magnetic performance as shown in Fig. 4. All the $Co_{50}Gd_{50-x}Ni_x$ amorphous alloys show a typical λ-shape within a broader temperature range as

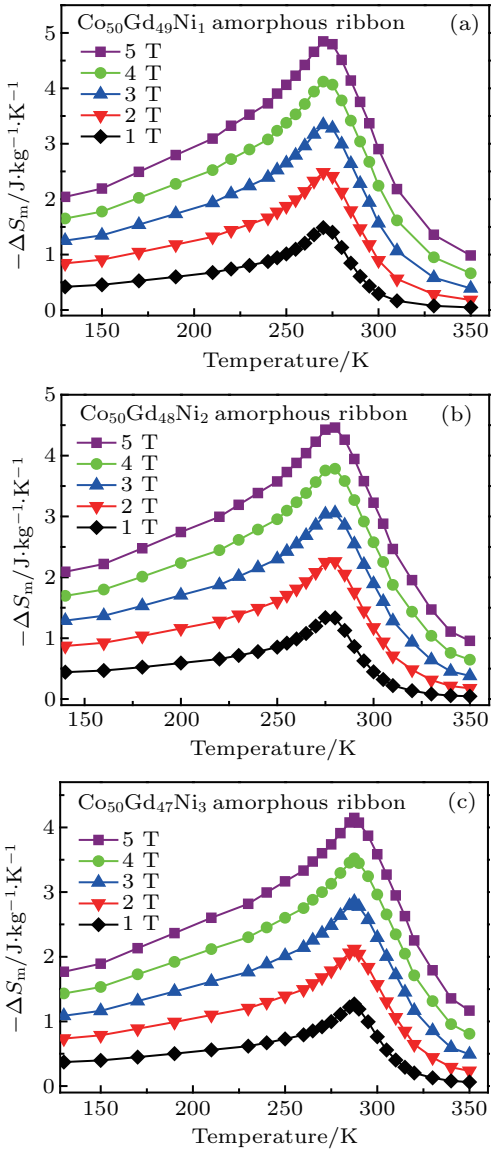


Fig. 4. The $-\Delta S_m$ vs. T curves for the $Co_{50}Gd_{50-x}Ni_x$ amorphous ribbons: (a) $x = 1$, (b) $x = 2$, and (c) $x = 3$.

listed in Table 1. The $-\Delta S_m^{peak}$ is increased to 4.9 J·kg^{-1}·K^{-1} for $Co_{50}Gd_{49}Ni_1$ compared with that of the $Co_{50}Gd_{50}$ amorphous alloy, and then decreased with continuous increase of the Ni content from 2 at.% to 3 at.%. This is anomalous because it is generally recognized from the relationship $-\Delta S_m^{peak} \propto T_C^{-2/3}$ that the $-\Delta S_m^{peak}$ in the Gd–TM-based amorphous alloys shows an approximately linear relationship with $T_C^{-2/3}$.[28] To investigate the relationship between $-\Delta S_m^{peak}$ and T_C of the $Co_{50}Gd_{50-x}Ni_x$ amorphous alloys in more detail, the relationship $-\Delta S_m^{peak}$ vs. $T_C^{-2/3}$ for each sample is plotted in Fig. 5. Unlike the previous results obtained from the Gd–TM-based metallic glasses, the dependence of $-\Delta S_m^{peak}$ on $T_C^{-2/3}$ for the $Co_{50}Gd_{50-x}Ni_x$ ($x = 0$, 1, 2, and 3) amorphous ribbons is somewhat like a superposition of a linearly decreasing and a parabolic-like relationship. The parabolic-like relationship between ΔS_m^{peak} and $T_C^{-2/3}$ is supposed to be resulted from the additional 3d–3d coupling from the interaction of Co–Ni, as the extra 3d–3d coupling is absent in the $Co_{50}Gd_{50}$ binary amorphous alloy and achieves the maximum effect in the $Co_{50}Gd_{49}Ni_1$ amorphous alloy. Consequently, T_C and $-\Delta S_m^{peak}$ of the binary $Gd_{50}Co_{50}$ metallic glass are improved simultaneously through 1 at.% Ni addition.

Table 1. Thermal, magnetic, and magnetocaloric properties of the $Co_{50}Gd_{50-x}Ni_x$ ($x = 1$, 2, and 3) and $Gd_{50}Co_{50}$ amorphous alloys.

Composition	T_g/K	T_x/K	ΔT_x/K	T_C						
$Co_{50}Gd_{50}$	507	557	50	267						
$Co_{50}Gd_{49}Ni_1$	529	579	50	273						
$Co_{50}Gd_{48}Ni_2$	523	571	48	280						
$Co_{50}Gd_{47}Ni_3$	538	558	20	289						
Composition	$-\Delta S_m^{peak}$/J·kg^{-1}·K^{-1}					ΔT_{ad}/K				
	1 T	2 T	3 T	4 T	5 T	2 T	5 T			
$Gd_{50}Co_{50}$	1.38	2.36	3.16	3.92	4.6	–	–			
$Co_{50}Gd_{49}Ni_1$	1.53	2.53	3.39	4.17	4.90	2.32	4.63			
$Co_{50}Gd_{48}Ni_2$	1.34	2.26	3.06	3.78	4.46	–	–			
$Co_{50}Gd_{47}Ni_3$	1.27	2.12	2.85	3.52	4.15	2.10	4.30			

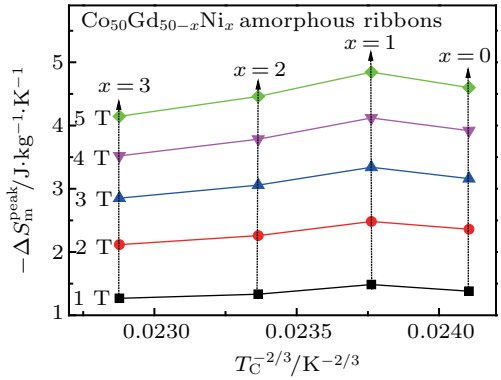


Fig. 5. The $-\Delta S_m^{peak}$ vs. $T_C^{-2/3}$ plots for the $Co_{50}Gd_{50-x}Ni_x$ ($x = 1$, 2, and 3) amorphous ribbons under various magnetic fields from 1 T to 5 T.

From another point of view, the cooling efficiency, as an important parameter of the magnetic refrigeration material, can be evaluated in a more intuitive way through considering the adiabatic temperature rise (ΔT_{ad}) of the alloys. By measuring the heat capacity $C_p(T)$ of the sample, as shown in the inset of Fig. 6, the adiabatic temperature rise (ΔT_{ad}) can be obtained as

$$\Delta T_{ad}(T, 0 \to H) = -\frac{T}{C_p(T)} \Delta S_m(T, 0 \to H).$$

Considering the $Co_{50}Gd_{49}Ni_1$ glassy ribbon with enhanced T_C and $-\Delta S_m^{peak}$, and the highest T_C among the $Co_{50}Gd_{50-x}Ni_x$ amorphous alloys, combined with the ΔS_m values of these samples, we calculate the ΔT_{ad} of $Co_{50}Gd_{49}Ni_1$ and $Co_{50}Gd_{47}Ni_3$ amorphous ribbons under the fields of 2 T and 5 T, as illustrated in the ΔT_{ad}–T curves in Fig. 6. The maximum ΔT_{ad} is about 2.32 K under 2 T and about 4.63 K under 5 T for the $Gd_{49}Co_{50}Ni_1$ amorphous ribbon, about 2.1 K under 2 T and about 4.3 K under 5 T for the $Gd_{47}Co_{50}Ni_3$ amorphous alloy. The maximum ΔT_{ad} of the two samples is superior to that of the Fe-based amorphous alloys under the same condition.[5–7,17,23,24]

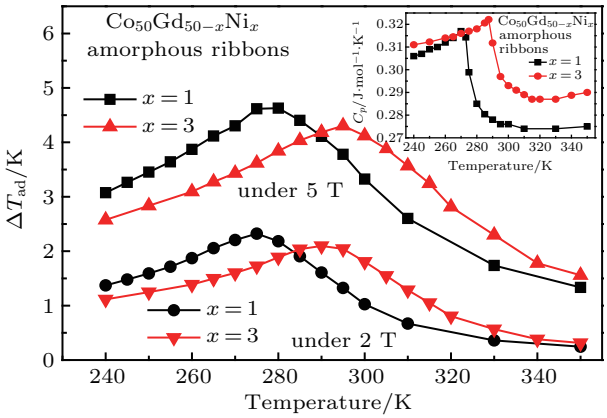


Fig. 6. The ΔT_{ad}–T curve of the $Co_{50}Gd_{49}Ni_1$ and $Co_{50}Gd_{47}Ni_3$ amorphous ribbons under the fields of 2 T and 5 T, the inset is the C_p–T curves of the amorphous alloys.

4. Conclusion

In summary, we added a small amount of Ni to $Gd_{50}Co_{50}$ binary amorphous alloy and obtained $Co_{50}Gd_{50-x}Ni_x$ ($x = 1$, 2, and 3) amorphous ribbons with improved Curie temperature. The glass forming ability remains stable under the substitution of 1 at.% Ni, while the substitution of 2–3 at.% Ni weakens the thermal stability and GFA of the alloy. The MCE of the $Co_{50}Gd_{50-x}Ni_x$ ($x = 1$, 2, and 3) amorphous alloys was studied. It was found that with the increasing T_C of the $Co_{50}Gd_{50-x}Ni_x$ amorphous alloys, $-\Delta S_m^{peak}$ increases to about 4.9 J·kg^{-1}·K^{-1} for $x = 1$, and then decreases to 4.46 J·kg^{-1}·K^{-1} for $x = 2$ and 4.15 J·kg^{-1}·K^{-1} for $x = 3$. The compositional dependence on the Curie temperature as well as $-\Delta S_m^{peak}$ of the $Co_{50}Gd_{50-x}Ni_x$ metallic glasses, and the mechanism involved, were investigated. It was believed that the improved T_C by minor Ni substitution for Gd, and the deviation of $-\Delta S_m^{peak}$ vs. $T_C^{-2/3}$ plots of the $Co_{50}Gd_{50-x}Ni_x$ ($x = 0$, 1, 2, and 3) amorphous alloys from the generally recognized linear relationship, are most likely due to the additional Co–Ni interaction.

References

[1] Phan M H and Yu S C 2007 *J. Magn. Magn. Mater.* **308** 325
[2] Brück E 2005 *J. Phys. D: Appl. Phys.* **38** R381
[3] de Oliveira N A and von Ranke P J 2010 *Phys. Rep.* **489** 89
[4] Gschneider Jr K A, Pecharsky V K and Tsokol A O 2005 *Rep. Prog. Phys.* **68** 1479
[5] Franco V, Blázquez J S, Ipus J J, Law J Y, Moreno-Ramírez L M and Conde A 2018 *Prog. Mater. Sci.* **93** 112
[6] Chen L S, Zhang J Z, Wen L, Yu P and Xia L 2018 *Sci. Chin.: Phys. Mech. Astro* **61** 056121
[7] Gan L H, Ma L Y, Tang B Z, Ding D and Xia L 2017 *Sci. Chin.: Phys. Mech. Astro* **60** 076121
[8] Luo Q and Wang W H 2010 *J. Alloys Compd.* **495** 209
[9] Du J, Zheng Q, Li Y B, Zhang Q, Li D and Zhang Z D 2008 *J. Appl. Phys.* **103** 023918
[10] Xia L, Chan K C, Tang M B and Dong Y D 2014 *J. Appl. Phys.* **115** 223904
[11] Xia L, Chan K C and Tang M B 2011 *J. Alloys Compd.* **509** 6640
[12] Fu H and Zou M 2011 *J. Alloys Compd.* **509** 4613
[13] Yuan F, Du J and Shen B L 2012 *Appl. Phys. Lett.* **101** 032405
[14] Tang B Z, Huang L W, Song M N, Ding D, Wang X and Xia L 2019 *J. Non-Cryst. Solids* **522** 119589
[15] Zhong X C, Huang X W, Shen X Y, Mo H Y and Liu Z W 2016 *J. Alloys Compd.* **682** 476
[16] Yu P, Zhang N Z, Cui Y T, Wu Z M, Wen L, Zeng Z Y and Xia L 2016 *J. Non-Cryst. Solids* **434** 36
[17] Tang B Z, Guo D Q, Ding D, Xia L and Chan K C 2017 *J. Non-Cryst. Solids* **464** 30
[18] Liu G L, Zhao D Q, Bai H Y, Wang W H and Pan M X 2016 *J. Phys. D: Appl. Phys.* **49** 055004
[19] Ma L Y, Gan L H, Chan K C, Ding D and Xia L 2017 *J. Alloys Compd.* **723** 197
[20] Song M N, Huang L W, Tang B Z, Ding D, Zhou Q and Xia L 2019 *Mod. Phys. Lett. B*
[21] Tang B Z, Yu P, Ding D, Wu C and Xia L 2017 *J. Magn. Magn. Mater* **424** 275
[22] Yu P, Chen L S and Xia L 2018 *J. Non-Crys. T Solids* **493** 82
[23] Wang Z W, Yu P, Cui Y T and Xia L 2016 *J. Alloys Compd.* **658** 598
[24] Xia L, Wu C, Chen S H and Chan K C 2015 *AIP Adv.* **5** 097122
[25] Wu C, Ding D, Xia L and Chan K C 2016 *AIP Adv.* **6** 035302
[26] Yuan C C, Yang F, Xi X K, Shi C L, Holland-Moritz D, Li M Z, Hu F, Shen B L, Wang X L, Meyer A and Wang W H 2020 *Mater. Today* **32** 26
[27] van der Marel D and Sawatzky G A 1988 *Phys. Rev. B* **37** 10674
[28] Belo J H, Amaral J S, Pereira A M, Amaral V S and Araújo J P 2012 *Appl. Phys. Lett.* **100** 242407